Anal. Chem. **2006,** *78,* 1485−1493

Nile Red-Adsorbed Gold Nanoparticle Matrixes for Determining Aminothiols through Surface-Assisted Laser Desorption/Ionization Mass Spectrometry

Yu-Fen Huang and Huan-Tsung Chang*

Department of Chemistry, National Taiwan University, 1, Section 4, Roosevelt Road, Taipei, Taiwan

This paper describes the use of Nile Red-adsorbed gold nanoparticles (NRAuNPs) as selective probes and matrixes for the determination of aminothiols through surface-assisted laser desorption/ionization mass spectrometry (SALDI-MS). The binding of three aminothiols—glutathione (GSH), cysteine (Cys), and homocysteine (HCys)—to the surfaces of these NRAuNPs induces their aggregation, which causes asubsequent changes in their color and fluorescence. Because arginine—a non-thiol amino acid—does not induce such aggregation, it is a straightforward process to use the NRAuNPs to selectively concentrate the aminothiols from a solution containing all four of these analytes; we were able to identify the three aminothiols in the precipitate, and arginine in the supernatant, directly through SALDI-MS measurements. Without using this preconcentration approach, the limits of detection (LODs) at a signal-to-noise ratio of 3 were 1.0, 2.0, and 1.3 μM for GSH, Cys, and HCys, respectively. In comparison, selective concentration using the NRAuNPs provided LODs of 25, 54, and 34 nM, for the determinations of GSH, Cys, and HCys, respectively. NRAuNP matrixes provide a number of advantages over the use of conventional organic matrixes (e.g., 2,5-dihydroxybenzoic acid), such as ease of preparation, selectivity, sensitivity, and repeatability. We validated the applicability of our method through the analyses of GSH in red blood cells and of Cys in plasma; we believe that this approach has great potential for diagnosis.

Matrix-assisted laser desorption/ionization mass spectrometry (MALDI-MS) rapidly became a powerful tool for biochemical analysis[1,2] after Karas and Hillemkamp introduced it in 1987.[3] As a result of rapid energy transfer from the UV-absorbing matrixes, the analytes undergo soft and efficient desorption/ionization with a minimum degree of fragmentation.[4−6] Although MALDI-MS is currently used successfully for the analyses of many varieties of nonvolatile and fragile molecules, especially proteins,[7] it has not been employed extensively for the characterization of low-molecular-weight compounds (<500), mainly because of the relatively high intensity of the matrix's background signals in the low-mass range. This disadvantage has hindered efforts to utilize the full power of MALDI-MS for high-throughput analyses of drugs and their metabolites from complex mixtures containing high concentrations of salts.[8−10]

The inhomogeneous cocrystallization of analytes with traditional organic matrixes, such as 2,5-dihydroxybenzoic acid (DHB) and sinapinic acid (SA), usually leads to the existence of "sweet spots" on the sample probe, which sometimes causes quantitative errors. To overcome this problem, much effort has been exerted to eliminate matrix ion interference and to improve sample homogeneity.[11−17] For example, surface-assisted laser desorption/ionization (SALDI) has been developed to use such systems as fine cobalt powders mixed with glycerol,[18] carbon powders,[19] and different inorganic matrixes[20,21] to assist in the LDI of analytes.

More recently, nanomaterials have become interesting SALDI matrixes because of their high surface areas, simple sample preparation techniques, flexibility of sample deposition under different conditions, and high UV absorptivity. Functionalized carbon nanomaterials, carbon nanotubes, silylated porous silicon, diamond nanoparticles, and gold nanoparticles (AuNPs) have been

* To whom correspondence should be addressed. Tel./Fax: 011-886-2-33661171. E-mail: changht@ntu.edu.tw.

(1) Harvey, D. J. *Mass Spectrom. Rev.* **1999**, *18*, 349−450.
(2) Fenselau, C.; Demirev, P. A. *Mass Spectrom. Rev.* **2001**, *20*, 157−171.
(3) Karas, M.; Hillenkamp, F. *Anal. Chem.* **1988**, *60*, 2299−2301.
(4) Alexander, M. L.; Hemberger, P. H.; Cisper, M. E.; Nogar, N. S. *Anal. Chem.* **1993**, *65*, 1609−1614.
(5) Glish, G. L.; Goeringer, D. E.; Asano, K. G.; McLuckey, S. A. *Int. J. Mass Spectrom. Ion Processes* **1989**, *94*, 15−24.
(6) Schlag, E. W.; Grotemeyer, J.; Levine, R. D. *Chem. Phys. Lett.* **1992**, *190*, 521−527.
(7) Canham, L. T. *Properties of Porous Silicon*; Institute of Electrical Engineers: London, 1997.
(8) Brown, R. S.; Lennon, J. J. *Anal. Chem.* **1995**, *67*, 1998−2003.
(9) Vestal, M. L.; Juhasz, P.; Martin, S. A. *Rapid Commun. Mass Spectrom.* **1995**, *9*, 1044−1050.
(10) Cohen, L. H.; Gusev, A. I. *Anal. Bioanal. Chem.* **2002**, *373*, 571−586.
(11) Vorm, O.; Roepstorff, P.; Mann, M. *Anal. Chem.* **1994**, *66*, 3281−3287.
(12) Nicola, A. J.; Gusev, A. I.; Proctor, A.; Jackson, E. K.; Hercules, D. M. *Rapid Commun. Mass Spectrom.* **1995**, *9*, 1164−1171.
(13) (a) Axelsson, J.; Hoberg, A.-M.; Waterson, C.; Myatt, P.; Shield, G. L.; Varney, J.; Haddleton, D. M.; Derrick, P. J. *Rapid Commun. Mass Spectrom.* **1997**, *11*, 209−213. (b) Hensel, R. R.; King, R. C.; Owens, K. G. *Rapid Commun. Mass Spectrom.* **1997**, *11*, 1785−1793.
(14) (a) Billeci, T. M.; Stults, J. T. *Anal. Chem.* **1993**, *65*, 1709−1716. (b) Gusev, A. I.; Wilkinson, W. R.; Proctor, A.; Hercules, D. M. *Anal. Chem.* **1995**, *67*, 1034−1041.
(15) Guo, Z.; Zhang, Q.; Zou, H.; Guo, B.; Ni, J. *Anal. Chem.* **2002**, *74*, 1637−1641.
(16) (a) Ayorinde, F. O.; Hambright, P.; Porter, T. N.; Keith, Q. L., Jr. *Rapid Commun. Mass Spectrom.* **1999**, *13*, 2474−2479. (b) Ayorinde, F. O.; Garvin, K.; Saeed, K. *Rapid Commun. Mass Spectrom.* **2000**, *14*, 608−615.
(17) (a) Zabet-Moghaddam, M.; Heinzle, E.; Tholey, A. *Rapid Commun. Mass Spectrom.* **2004**, *18*, 141−148. (b) Li, Y. L.; Gross, M. L.; Hsu, F.-F. *J. Am. Soc. Mass Spectrom.* **2005**, *16*, 679−682.

10.1021/ac0517646 CCC: $33.50
Published on Web 01/05/2006

used for the mass spectrometric analyses of small analytes, such as peptides, and large molecules, such as proteins.[20d,22−27] There is also interest in integrating the separation and the mass spectrometric detection of biomolecules, such as peptides, through the use of nanomaterials.[20b,d,22,23b,24,26,27] AuNPs and gold-modified magnetic Fe_3O_4 nanoparticles have been used to selectively concentrate positively charged peptide residues from the tryptic digest products of cytochrome *c* through Columbic interactions.[25] The flocculated and trapped mixtures were then mixed separately with traditional matrixes, such as SA and DHB, for their MS analyses. With the advantage of preconcentration, this approach allows the MALDI-MS detection of low concentrations (10^{-7} M) of such peptides. MALDI-MS has also been applied to study the surface adsorption of organomercaptans on AuNPs and to the detection of Au−peptide mixtures blended with DHB.[28] When using 2−10-nm-diameter AuNPs as SALDI matrixes, a number of peptides, such as substance P, and small proteins, such as bovine insulin, were detectable through MS.[29] With $\sim 10^7-10^9$ bound analyte molecules per AuNP, a highly efficient ionization process for AuNPs can be achieved; the AuNPs may possess the capacity to ionize more than one analyte per laser pulse or have the potential to regenerate their matrix-"active" state between laser pulses. That study also suggested that AuNP matrixes afford a degree of selectivity: the preferential ionization of phosphotyrosine-containing peptides occurred over phosphoserine- or phosphothreonine-containing ones. Signals deriving from Au clusters are usually detected when AuNPs are used as matrixes; this phenomenon allows the mass spectrometric investigation of Au−SR clusters.[30]

Although AuNPs with DHB and AuNPs have been used successfully as MALDI and SALDI matrixes for the detection of molecules having masses above 1000 g/mol, to the best of our knowledge the detection of small molecules, such as aminothiols, has yet to be reported. The determination of aminothiols in biological samples, such as blood, is extremely important because they play several important roles in metabolism and homeostasis. For example, glutathione (GSH), the most abundant non-protein tripeptide present in cells, plays numerous physiological roles, including maintaining the balance between oxidation and antioxidation.[31] In addition, the metabolic disturbances of aminothiols are related to several diseases, such as vascular disorder and arteriosclerosis.[32−35] The cysteine (Cys) content in urine increases in cases of cystinuria, which is the most common inherited defect of amino acid transport (the overall prevalence is 1 in 7000).[33] Elevated levels of plasma homocysteine (HCys) is a known risk for atherosclerotic vascular disease.[36]

Our goal in this study was to determine whether Nile Red (NR)-adsorbed AuNPs (NRAuNPs) could be used as SALDI matrixes for the mass spectrometric determination of aminothiols. Applying a dual assay based on colorimetric and fluorescence changes allowed us to use NRAuNPs to differentiate between positively and negatively charged and neutral aminothiols.[37] Thus, we believed that conducting SALDI-MS using NRAuNPs would improve the selectivity for aminothiols. We carefully evaluated the effects that a number of parameters, such as the concentrations and sizes of NRAuNPs, the pH, and the laser fluence, have on the sensitivity of the SALDI-MS detection of GSH, Cys, and HCys. Finally, we applied our proposed method to the successful determination of the aminothiols in human lysed red blood cells and in blood plasma; this approach has the advantages of simplicity, selectivity, sensitivity, and repeatability.

EXPERIMNETAL SECTION

Chemicals. Sodium tetrachloroaurate(III) dihydrate and GSH were obtained from Sigma (St. Louis, MO). Citric acid, Cys, HCys, DHB, and trisodium citrate were purchased from Aldrich (Milwaukee, WI). NR, arginine, acetonitrile (ACN), dimethyl sulfoxide (DMSO), hydrochloric acid, and ammonium hydroxide were obtained from Acros (Geel, Belgium). Citrate solutions were prepared using either trisodium citrate or citric acid. The values of pH of the 0.5 mM citrate solutions, which were prepared from mixtures of trisodium citrate solutions (100 mM) and HCl (2.0 M), ranged from 3.0 to 6.0. When 100 mM citric acid was used to prepare citrate solution (0.5 mM), NH_4OH (25−30%) was used to adjust the pH to 4.0.

Synthesis of 14-, 32-, and 56-nm-Diameter AuNPs. Three charges of trisodium citrate (1%; 0.8, 0.5, and 0.3 mL) were added rapidly to three aliquots, respectively, of 0.01% $NaAuCl_4$ (50 mL) that were heated under reflux.[38,39] The solutions were heated

(18) Tanaka, K.; Waki, H.; Ido, Y.; Akita, S.; Yoshida, Y. *Rapid Commun. Mass Spectrom.* **1988**, *2*, 151−153.
(19) (a) Sunner, J.; Dratz, E.; Chen, Y.-C. *Anal. Chem.* **1995**, *67*, 7, 4335−4342. (b) Chen, Y.-C.; Tsai, M.-F. *J. Mass Spectrom.* **2000**, *35*, 1278−1284. (c) Wu, J.-Y.; Chen, Y.-C. *J. Mass Spectrom.* **2002**, *37*, 85−90. (d) Dale, M. J.; Knochenmuss, R.; Zenobi, R. *Anal. Chem.* **1996**, *68*, 3321−3329.
(20) (a) Wei, J.; Buriak, J. M.; Siuzdak, G. *Nature* **1999**, *399*, 243−246. (b) Shen, Z.; Thomas, J. J.; Averbuj, C.; Broo, K. M.; Engelhard, M.; Crowell, J. E.; Finn, M. G.; Siuzdak, G. *Anal. Chem.* **2001**, *73*, 612−619. (c) Go, E. P.; Prenni, J. E.; Wei, J.; Jones, A.; Hall, S. C.; Witkowska, H. E.; Shen, Z.; Siuzdak, G. *Anal. Chem.* **2003**, *75*, 2504−2506. (d) Trauger, S. A.; Go, E. P.; Shen, Z.; Apon, J. V.; Compton, B. J.; Bouvier, E. S. P.; Finn, M. G.; Siuzdak, G. *Anal. Chem.* **2004**, *76*, 4484−4489. (e) Kruse, R. A.; Li, X.; Bohn, P. W.; Sweedler, J. V. *Anal. Chem.* **2001**, *73*, 3639−3645.
(21) Kinumi, T.; Saisu, T.; Takayama, M.; Niwa, H. *J. Mass Spectrom.* **2000**, *35*, 417−422.
(22) Ugarov, M. V.; Egan, T.; Khabashesku, D. V.; Schultz, J. A.; Peng, H.; Khabashesku, V. N.; Furutani, H.; Prather, K. S.; Wang, H.-W. J.; Jackson, S. N.; Woods, A. S. *Anal. Chem.* **2004**, *76*, 6734−6742.
(23) (a) Xu, S.; Li, Y.; Zou, H.; Qiu, J.; Guo, Z.; Guo, B. *Anal. Chem.* **2003**, *75*, 6191−6195. (b) Chen, W.-Y.; Wang, L.-S.; Chiu, H.-T.; Chen, Y.-C.; Lee, C.-Y. *J. Am. Soc. Mass Spectrom.* **2004**, *15*, 1629−1635.
(24) Kong, X. L.; Huang, L. C. L.; Hsu, C.-M.; Chen, W.-H.; Han, C.-C.; Chang, H.-C. *Anal. Chem.* **2005**, *77*, 259−265.
(25) Teng, C.-H.; Ho, K.-C.; Lin, Y.-S.; Chen, Y.-C. *Anal. Chem.* **2004**, *76*, 4337−4342.
(26) Chen, C.-T.; Chen, Y.-C. *Anal. Chem.* **2005**, *77*, 5912−5919.
(27) Chou, P.-H.; Chen, S.-H.; Liao, H.-K.; Lin, P.-C.; Her, G.-R.; Lai, A. C.-Y.; Chen, J.-H.; Lin, C.-C.; Chen, Y.-J. *Anal. Chem.* **2005**, *77*, 5990−5997.
(28) Kirk, J. S.; Bohn, P. W. *J. Am. Chem. Soc.* **2004**, *126*, 5920−5926.
(29) McLean, J. A.; Stumpo, K. A.; Russell, D. H. *J. Am. Chem. Soc.* **2005**, *127*, 5304−5305.
(30) (a) Schaaff, T. G.; Shafigullin, M. N.; Khoury, J. T.; Vezmar, I.; Whetten, R. L. *J. Phys. Chem. B* **2001**, *105*, 8785−8796. (b) Schaaff, T. G. *Anal. Chem.* **2004**, *76*, 6187−6196.
(31) Wu, G.; Fang, Y.-Z.; Yang, S.; Lupton, J. R.; Turner, N. D. *J. Nutr.* **2004**, *134*, 489−492.
(32) McCully, K. S. *Am. J. Pathol.* **1969**, *56*, 111−128.
(33) Mudd, S. H.; Levy, H. L.; Skovby, F. In *The Metabolic and Molecular Basis of Inherited Disease*; Scriver, C. R., Beaudet, A. L., Sly, W. S., Valle, D., Eds.; McGraw-Hill: New York, 1995; pp 1279−1328.
(34) Danesh, J.; Lewington, S. *J. Cardiovasc. Risk* **1998**, *5*, 229−232.
(35) Jacob, N.; Bruckert, E.; Giral, P.; Foglietti, M. J.; Turpin, G. *Atherosclerosis* **1999**, *146*, 53−59.
(36) Boushey, C. J.; Beresford, S. A. A.; Omenn, G. S.; Motulsky, A. G. *J. Am. Med. Assoc.* **1995**, *274*, 1049−1057.
(37) Chen, S.-J.; Chang, H.-T. *Anal. Chem.* **2004**, *76*, 3727−3734.
(38) Frens, G. *Nat., Phys. Sci.* **1973**, *241*, 20−22.
(39) Grabar, K. C.; Freeman, R. G.; Hommer, M. B.; Natan, M. J. *Anal. Chem.* **1995**, *67*, 735−743.

under reflux for an additional 8 min, during which time the colors changed to wine-red, deep-red, and pale-red, respectively. The solutions were set aside to cool to room temperature; they were stable for at least 6 months. In this paper, the concentrations of the as-prepared AuNPs are each denoted as 1×; they correspond to concentrations of about 2.4×10^{12}, 1.6×10^{11}, and 3.0×10^{10} particles/mL for the 14-, 32-, and 56-nm-diameter AuNPs, respectively.[40]

Characterization of AuNPs. A double-beam UV−visible spectrophotometer (Cintra 10e) obtained from GBC (Victoria, Australia) was used to measure the absorbance of the AuNPs in citrate solutions. For the 14-, 32-, and 56-nm-diameter AuNPs, the UV−visible absorption measurements (not shown) indicated that the maximum wavelengths of the surface plasmon resonance were 518, 526, and 535 nm, respectively; these values are consistent with the expected sizes of the AuNPs. The sizes and their distribution (±2.0%) were further confirmed through transmission electron microscopy (TEM) measurements using an H7100 TEM from Hitachi (Tokyo, Japan) operated at 75 kV. All spectrometric measurements were conducted using a fluorometer (Aminco-Bowman; ThermoSpectronic, Pittsford, NY) operated through excitation at 480 nm and emission at 610 nm.

Preparation of NRAuNPs. A stock solution of NR (1.0 mM) was prepared in DMSO. Three aliquots of NR solutions (5.0 μL each) were added separately to 14-, 32-, and 56-nm-dianeter AuNP solutions (1× ; 5.0 mL each) that were prepared in 0.5 mM citrate (pH 4.0). The solutions were equilibrated at ambient temperature and pressure overnight and then subjected to three cycles of centrifugation at 12 000 rpm (relative centrifugal force, 16400*g*) for 10 min and washing with citrate solution (5.0 mL). Finally, the precipitates were resuspended in 0.5 mM citrate solution (pH 4.0). The as-prepared solutions are denoted as NRAuNPs, and for simplicity, their concentrations are all presented as 1×. The 14-nm-diameter NRAuNPs were then concentrated by centrifugation at 12 000 rpm for 10 min. The concentration (30×) of the concentrated 14-nm-diameter NRAuNPs was estimated from the ratio of its absorbance value at 518 nm to that of the 1× NRAuNPs.[41]

Preparation of Samples. Unless otherwise noted, 14-nm-diameter NRAuNPs were used. The model aminothiols (5.0 μL; 0.1 mM−0.1 M) were added separately to different concentrations (0.5−10× ; 0.5 mL each) of both NRAuNP and AuNP solutions and equilibrated for 1 h. Samples of the flocculated mixtures or supernatants (~2.0 μL) were pipetted into a stainless steel 384-well MALDI target (Bruker Daltonics). For control experiments, the solutions consisting of aminothiols and NRAuNPs or AuNPs were subjected to four cycles of centrifugation (6000 rpm; 10 min) and washing (0.5 mM citrate; 0.5 mL); the supernatants were then pipetted into a stainless steel 384-well MALDI target and dried in air at room temperature prior to SALDI-MS measurements. In the cases where DHB (20 mg/mL in water) was used as a comatrix for MALDI-MS analysis, DHB (1.0 μL) was mixed with the flocculated mixtures or supernatants (1.0 μL). The mixtures were then pipetted into the wells of the steel plate and dried in air at room temperature prior to MALDI-MS or SALDI-MS measurements.

Preparation of Thiol Extracts from Lysed Red Blood Cells (RBCs) and Plasma Samples. Whole blood samples from an apparently healthy female adult were collected into K_2 EDTA Vacutainer blood collection tubes (Becton Dickinson, Franklin Lakes, NJ). Fresh blood samples (0.5 mL) were diluted to 1.0 mL using phosphate-buffered saline (PBS) that consists of 37.0 mM phosphate (pH 7.4) and 38.0 mM sodium chloride. After four cycles of centrifugation at 2500 rpm for 10 min and washing with PBS (1.0 mL) at room temperature, the cell pellets were lysed in ammonium citrate buffer (0.5 mM, pH 4.0; 1.0 mL) and then the proteins were removed by using 80% ACN. The NRAuNPs (final concentration, 3×) were added to the deproteined RBC lysates, and the mixtures were incubated at room temperature for 1 h. The (NR)AuNP/thiol mixtures were then subjected to four cycles of centrifugation at 6000 rpm for 10 min and washing with ammonium citrate (0.5 mM, pH 4.0; 1.0 mL). The pellets were then redispersed in 0.5 mM ammonium citrate (pH 4.0; 1.0 mL). To obtain plasma samples, the collected whole blood samples were immediately centrifuged at 2500 rpm for 10 min at room temperature. The plasma samples were stored at −20 °C. The same procedures were performed to obtain the (NR)AuNP:thiol mixtures of the plasma samples.

MALDI-TOF and SALDI-TOF MS Measurements. Mass spectrometry experiments were performed in the positive-ion mode on a reflectron-type time-of-flight (TOF) mass spectrometer (Biflex III, Bruker) equipped with a 1.25-m flight tube. The samples were irradiated with a 337-nm-diameter nitrogen laser at 10 Hz (pulse duration, 4 ns). Ions produced by laser desorption were stabilized energetically during a delayed extraction period of 200 ns and then accelerated through the linear TOF reflection before entering the mass analyzer. The available accelerating voltages existed in the range from +20 to −20 kV. To obtain good resolution and signal-to-noise (S/N) ratios, the laser fluence was adjusted to slightly higher than the threshold and each mass spectrum was generated by averaging 300 laser pulses.

RESULTS AND DISCUSSION

NRAuNPs as Assisted Matrixes for SALDI-MS Analysis. Once the aminothiol molecules (GSH, Cys, or HCys) bound to the NRAuNPs, the NR products were released into the bulk solution, as exhibited in Scheme 1A. As a result, the fluorescence intensity of the solution increased dramatically at a wavelength of 610 nm (excitation wavelength, 480 nm).[37] In this paper, we denote the aminothiol (RNHR′SH)-adsorbed (NR)AuNPs as "(NR)-AuNP/SR′NHR." We do not call them "AuNP/SR′NHR" because we could not rule out the possibility of some NR species remaining on the AuNP surface; thus, the term "(NR)AuNP/SR′NHR" encompasses the presence of both (NR)AuNP/SR′NHR and AuNP/SR′NHR. Aminothiols present at high concentrations (>7.5 μM) immediately induced aggregation of AuNP/SR′NHR, but color changes at low concentrations (<5.0 μM) were induced slowly. When we added non-thiol molecules, such as arginine (10 μM), to the solution, we did not observe any significant changes in either the color or fluorescence intensity (Scheme 1B).

The aminothiols molecules bound selectively to the (NR)-AuNPs, which minimized the interference from other solutes, such as citrate, NR, the NR product, and salts, when conducting SALDI-MS measurements of the flocculated mixtures. To test our hypothesis and the possibility of using AuNPs as matrixes, we

(40) Jana, N. R.; Gearheart, L.; Murphy, C. J. *Langmuir* **2001**, *17*, 6782−6786.
(41) Huang, M.-F.; Kuo, Y.-C.; Huang, C.-C.; Chang, H.-T. *Anal. Chem.* **2004**, *76*, 192−196.

Scheme 1

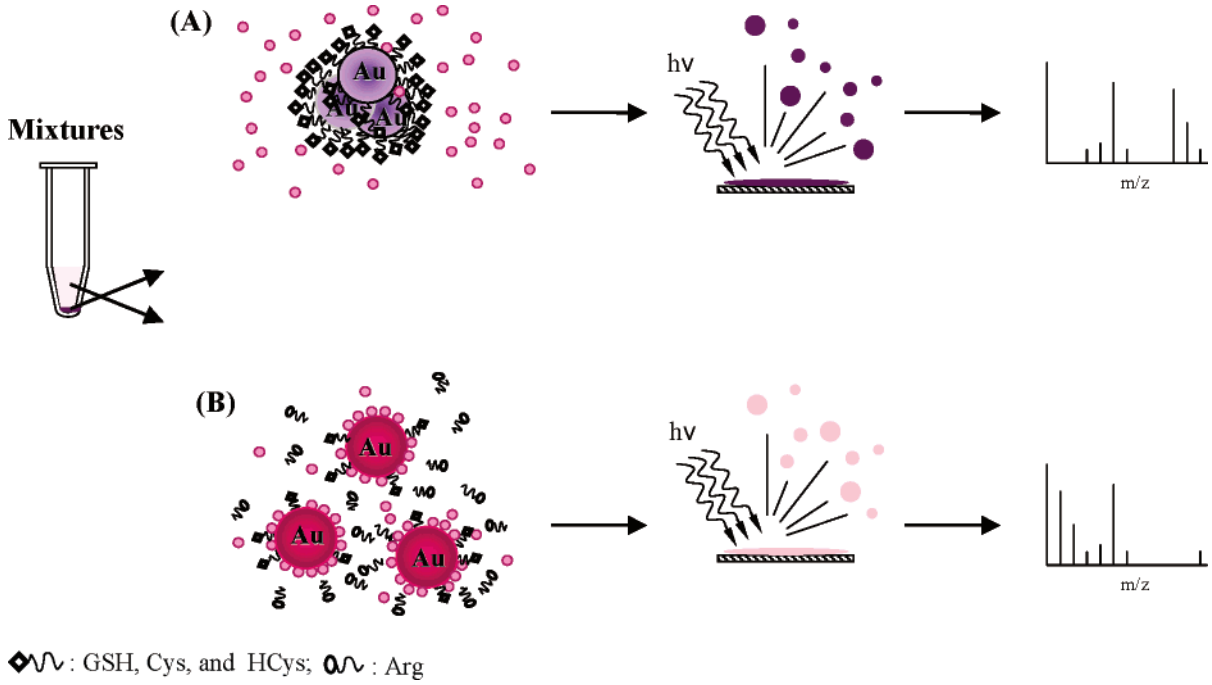

conducted SALDI-MS using GSH (1 mM) as a representative analyte.[29] Figure 1A indicates that we could detect peaks at *m/z* 330.07, 352.05, 374.04, 346.03, and 368.02 for $[GSH + Na]^+$, $[GSH - H + 2Na]^+$, $[GSH - 2H + 3Na]^+$, $[GSH + K]^+$, and $[GSH - H + 2K]^+$, respectively, in the corresponding mass spectrum.[18,19a,d,23a,42] To clarify the roles played by the AuNPs and the NR molecules remaining on the AuNP surface during the SALDI of GSH, we performed SALDI-MS measurements using AuNPs as a control. From UV−visible absorption measurements performed at 610 nm, we note that GSH bound to the NRAuNPs and the AuNPs to the same extent. Figure 1B indicates that we obtained a similar mass spectrum, but with lower intensities, suggesting that NR has only a minor effect on the SALDI efficiency. In both cases, we readily detected the Na^+ and K^+ adduct ions of GSH under a low laser fluence (43.5 μJ); this result is similar to that obtained when using a conventional "chemical" matrix such as DHB. It is likely that energy transfer from the AuNPs to the analyte occurred through a thermally driven process, similar to the mechanism proposed by Tanaka.[18] The strong adsorption bands of the (NR)AuNPs throughout the near-UV to near-IR ranges suggest that the (NR)AuNPs have an advantage of over conventional chemical matrixes when used in SALDI.[43] When conducting the SALDI-MS measurements of the supernatant, the small peak that we detected at *m/z* 330.07 (~20-fold less intense than that in Figure 1A) suggests that there were small amounts of (NR)AuNP/GS. GSH, or both in the supernatant. To support this hypothesis, we subjected the solution to four cycles of centrifugation and washing; Figure 1C indicates that after such treatment we could detect no peaks corresponding to GSH. After four cycles of centrifugation and washing, we estimate that the concentrations of free GSH in the solution, which were originally ~0.9 mM (predisplacement), were below 0.09 nM in the solution used to prepare the SALDI samples. These results suggest that centrifugation is necessary to achieve better sensitivity. Figure 1D indicates that low signal intensities, greater matrix interference, and poor repeatability occurred when we conducted MS measurements using the (NR)AuNP/GS + DHB mixture; most likely this situation arose because of the poor crystallization of DHB with GSH in the presence of (NR)AuNP. When using

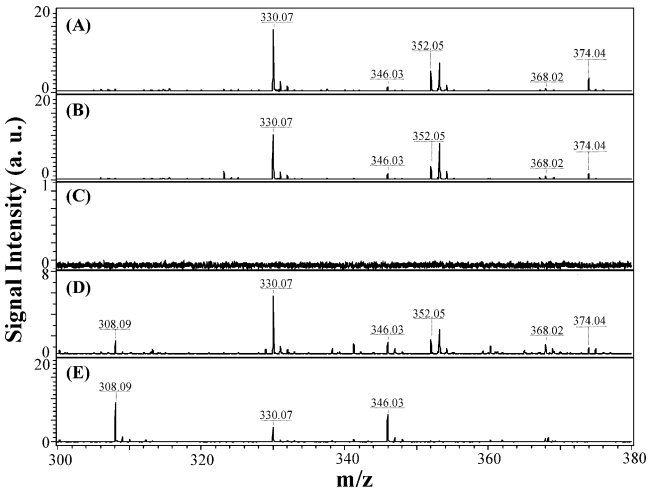

Figure 1. Mass spectra of GSH (A, B) 14-nm-diameter (NR)AuNPs (1×) and 14-nm-diameter AuNPs, respectively, used as matrixes. (C) Mass spectrum of the supernatant of mixtures containing GSH and (NR)AuNPs after four cycles of centrifugation and washing. (D) (NR)-AuNPs (1×) and DHB (10 mg/mL) were used as matrixes. (E) DHB (10 mg/mL) was used as matrix. The concentrations of GSH are (A−D) 1.0 and (E) 5 mM, respectively. The peaks at *m/z* 308.09, 330.07, 352.05, and 374.04, 346.03, and 368.02 are assigned respectively to the $[GSH + H]^+$, $[GSH + Na]^+$, $[GSH - H + 2Na]^+$, $[GSH - 2H + 3Na]^+$, $[GSH + K]^+$, and $[GSH - H + 2K]^+$ ions. A total of 300 pulsed laser shots were applied under a laser fluence set at 52.5 μJ.

(42) Zhang, Q.; Zou, H.; Guo, Z.; Zhang, Q.; Chen, X.; Ni, J. *Rapid Commun. Mass Spectrom.* **2001**, *15*, 217−223.
(43) Schurenberg, M.; Dreisewerd, K.; Hillenkamp, F. *Anal. Chem.* **1999**, *71*, 221−229.

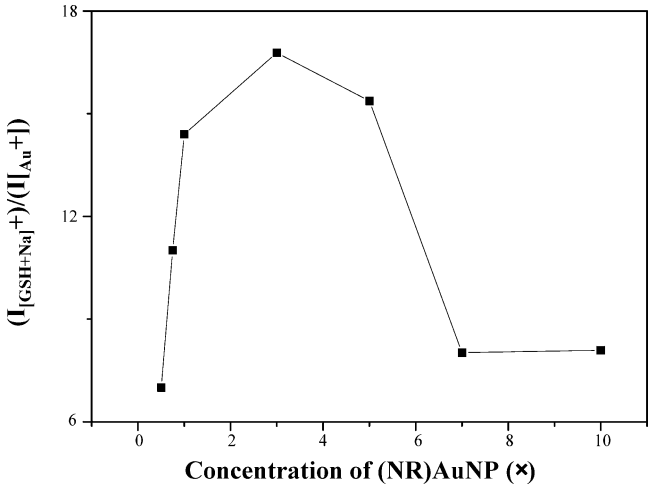

Figure 2. Intensity ratios of the $[GSH + Na]^+$ and $[Au]^+$ ions plotted against the concentration (0.5−10×) when using the 14-nm-diameter (NR)AuNPs as sample matrixes. The concentration of GSH was 1.0 mM.

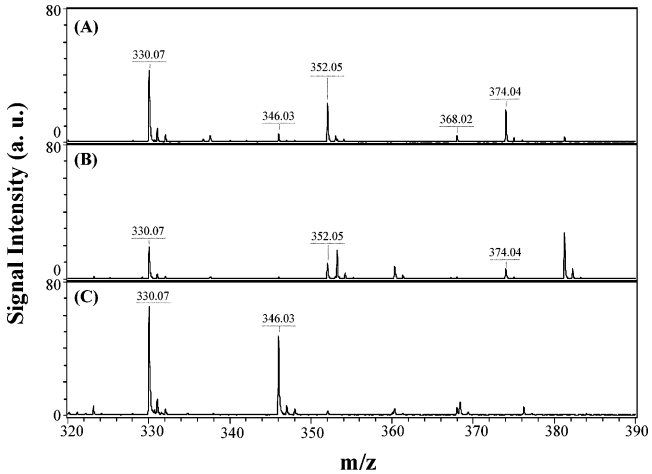

Figure 3. Mass spectra of GSH (0.1 mM) at different values of pH when using the 14-nm-diameter (NR)AuNPs (3×) as matrixes. (A, B) The 14-nm-diameter (NR)AuNPs (3×) were prepared in 0.5 mM citrate solutions at pH 4.0 and 6.0, respectively. The values of pH of the trisodium citrate solution were adjusted using HCl. (C) The citrate solution (pH 4.0) was prepared by mixing citric acid and NH_4OH. The peaks at *m*/*z* 330.07, 352.05, and 374.04 are assigned respectively to the $[GSH + Na]^+$, $[GSH - H + 2Na]^+$, and $[GSH - 2H + 3Na]^+$ ions; the peaks at *m*/*z* 346.03 and 368.02, are that of the $[GSH + K]^+$ and $[GSH - H + 2K]^+$ions.

DHB as matrixes, we experienced poor sensitivity and irreproducible results. Figure 1E exhibits that the peak at *m*/*z* 330.07 for GSH (5 mM) is smaller when GSH was mixed with DHB than that exhibited in Figure 1A.

Effects of Particle Size and Concentration. The number of adsorbed analyte molecules and the electrical and optical properties of the (NR)AuNPs are strongly dependent on the particle size. Thus, we expected to observe different SALDI efficiencies (sensitivities) for aminothiols when using differently sized NRAuNPs as selective probes and SALDI matrixes. In this study, we tested (NR)AuNPs of three different sizes (14-, 32-, and 56-nm diameters) for their use in the analysis of GSH through SALDI-MS. When we used the 32- and 56-nm-diameter (NR)AuNPs, the intensities of the signal for the $[GSH + Na]^+$ ions were about 86 and 11%, respectively, of that obtained when using the 14-nm-diameter (NR)-AuNPs. Although the adsorbed GSH molecules were present at 2.4×10^4, 3.5×10^5, and 1.8×10^6 molecules per 14-, 32-, and 56-nm-diameter AuNP, respectively, their concentrations in the solutions were 2.4×10^{12}, 1.6×10^{11}, and 3×10^{10} particles/mL, respectively. One interesting finding is that the intensities of the $[Au_n]^+$ ions ($n = 1-3$) were higher when using the greater-sized NRAuNPs. For example, the intensities of these signals when using the 32-nm-diameter (NR)AuNPs were about twice as high as those obtained when using the 14-nm-diameter (NR)AuNPs. Thus, we conclude that use of the 14-nm-diameter NRAuNPs is preferable because they provide the greater S/N ratios. Our results are similar to those reported by McLean et al., who found that the relative signal intensities of the peptide to those for $[Au_n]^+$ ($n = 3$ and 5) were 1.1 and 0.7 when using 2- and 10-nm-diameter AuNPs, respectively.[29]

Next, we tested the effects that the concentrations of the 14-nm-diameter (NR)AuNPs (0.5−10×) have on the signal intensities of GSH (1 mM). Figure 2 indicates that the ratio of the signals of the $[GSH + Na]^+$ and $[Au]^+$ ions was maximized when using the 3× (NR)AuNPs Although the intensity of the analyte ion signal (*m*/*z* 330.07) decreased only slightly upon increasing the (NR)-AuNP concentration, the loss in mass resolution and the stronger $[Au_n]^+$ background signals became problematic at concentrations higher than 3×. When using the 3× (NR)AuNPs, we found that the signals of the analyte ion and the quality of the MS spectra remained almost the same when the GSH concentration was above 0.05 mM. We note that the fluorescence measurements indicated that the adsorption of GSH was saturated at a GSH concentration of 0.05 mM.[37] This finding suggests that the analyte signals arose only from molecules adsorbed on the particle surface; this result coincides with the findings described by Schurenberg et al.[43]

Effects of pH and Choice of Buffer Solution. According to a previous study (a dual assay based on colorimetric and fluorescence changes), we found that the efficiency of the displacement of the NR product from the (NR)AuNP surface by GSH (pI = 2.86) increased upon decreasing the value of pH of the citrate solution from 9.0 to 4.0.[37] The signals are greater at pH 4.0 (Figure 3A) than those at pH 6.0 (Figure 3B). When using (NR)AuNPs as SALDI matrixes for MS measurements performed in the positive ion mode, a low pH is favorable in terms of the greater ionization efficiencies.[44] This situation is also due to a greater displacement capability of GSH at lower pH. Upon decreasing the pH, the degree of Coulombic repulsion reduced as a result of decreasing the negative charge densities of both the (NR)AuNP surface [citrate-stabilized (NR)AuNPs] and GSH. We note that the (NR)AuNPs were not stable at values of pH below 4.0; we observed poor sensitivity and reproducibility.

The presence of chemical species,[45,46] salts,[47] and organic solvents[48] in aqueous solution all have great effects on the sensitivity of SALDI-MS analyses. To minimize the formation of

(44) Krüger, R.; Pfenninger, A.; Fournier, I.; Glückmann, M.; Karas, M. *Anal. Chem.* **2001**, *73*, 5812−5821.
(45) Cohen, S. L.; Chait, B. T. *Anal. Chem.* **1996**, *68*, 31−37.
(46) Yao, J.; Scott, J. R.; Young, M. K.; Wilkins, C. L. *J. Am. Soc. Mass Spectrom.* **1998**, *9*, 805−813.
(47) Liao, P.-C.; Allison, J. *J. Mass Spectrom.* **1995**, *30*, 408−423.
(48) Figueroa, I. D.; Torres, O.; Russell, D. H. *Anal. Chem.* **1998**, *70*, 4527−4533.

the multiply sodiated GSH adducts, which had a detrimental effect on the resolution and sensitivity, we tested use of a citrate solution (pH 4.0) that we prepared from citric acid and NH_4OH. Figure 3C indicates that only two major peaks appear in the MS spectrum; they correspond to the $[GSH + Na]^+$ and $[GSH + K]^+$ adduct ions. As a result of the presence of fewer species of sodiated GSH adduct ions, the peak height for the $[GSH + Na]^+$ ion is greater (~1.5-fold) than that exhibited in Figure 3A. Even though it has been suggested that the presence of metal ions is preferred for most inorganic particle-catalyzed SALDI-MS analyses,[18,19a,d,23a,42] details of the cationization process remains under investigation.

Quantitative Analyses of Three Model Thiols. SALDI-MS quantification is generally considered to be an unreliable procedure because of poor intra- (sample-to-sample) and inter-sample (spot-to-spot and shot-to-shot signal) experimental reproducibility. In this study, we compared the quantitative results of the MS analyses of GSH, Cys, and HCys when using either (NR)AuNPs as the SALDI matrix or DHB as the MALDI matrix. When using the (NR)AuNPs, we observed that the intensities of the (Na, K) GSH adduct ions, as well as those of the protonated and (Na, K) Cys and HCys adduct ions, varied to within less than 10−20% over 50 sample spots; in contrast, these variations were greater than 60% when using DHB.[49] Figure 4 shows that when the (NR)AuNPs were used as the SALDI matrix, the changes in the peak heights were linear with respect to the concentrations of the three model aminothiols. The correlation coefficients (R^2) were 0.997, 0.996, and 0.995 for the determinations of GSH, Cys, and HCys in the concentration ranges 2.5−50, 5.0−75, and 2.5−100 μM, respectively. The limits of detection (LODs) for GSH, Cys, and HCys at a S/N ratio of 3 were 1.0, 2.0, and 1.3 μM, respectively. Our results are comparable with those of other reported data; the LODs for amino acids and HCys ranged from submicromolar to several micromolar when using MALDI-MS.[50] We point out that using (NR)AuNPs as SALDI matrixes provides a potentially precise and time-saving procedure for the quantitative assays of aminothiols; it obviates the need to conduct calibrations using internal standards.

We also tested the detection of 5.0 μM GSH through MALDI-MS using DHB as a matrix, but it was difficult to assign the corresponding peaks mainly because of the presence of high-intensity background signals (results not shown). The slightly improved sensitivity when using nanoparticles as matrixes is the result of the greater molar matrix-to-analyte ratio: $\sim 10^2-10^4$ analytes/particles versus 10^3-10^5 matrix molecules/analyte. The highly efficient ionization process that occurred when using the (NR)AuNPs may arise because the AuNPs have the capacity to ionize more than one analyte per laser pulse or because they have the potential to regenerate to a matrix-"active" state between each laser pulse.[29] Using (NR)AuNPs as SALDI matrixes provides further advantages over DHB, including easy sample preparation and fewer problems associated with inhomogeneity of the mixture.

In a previous paper, we reported the high sensitivity of NRAuNPs for the detection of GSH, Cys, and HCys through colorimetric and fluorescence changes, but these dual assays offer limited selectivity for the three model analytes. By taking advantage of the selectivity of the MS technique, we used the NRAuNPs to analyze simultaneously an aqueous solution containing the three analytes. The MS spectra of the three analytes are depicted in Figure 5A (Cys and HCys) and B (GSH). In Figure 5A, we assign the peaks at m/z 121.99, 143.98, and 159.96 to $[Cys + H]^+$, $[Cys + Na]^+$, and $[Cys + K]^+$, respectively, and those at m/z 136.01, 158.00, and 173.98 to $[HCys + H]^+$, $[HCys + Na]^+$, and $[HCys + K]^+$, respectively. In contrast to GSH, we detected both protonated and (Na, K) adduct ions for Cys and HCys. The sodiated ions, such as $[Cys + Na]^+$ and $[HCys + Na]^+$ at m/z 143.98 and 158.00, dominated at low laser fluences, whereas at laser fluences above 57.0 μJ, we clearly observed higher intensities for the signals of the $[Cys + H]^+$ and $[HCys + H]^+$ ions. Higher laser fluences were required to obtain greater signals for the $[Cys + H]^+$ and $[HCys + H]^+$ ions because Cys and HCys have lower proton affinities.[51] The relative peak intensities of the three model analytes (Figure 5) reflect the higher desorption or ionization

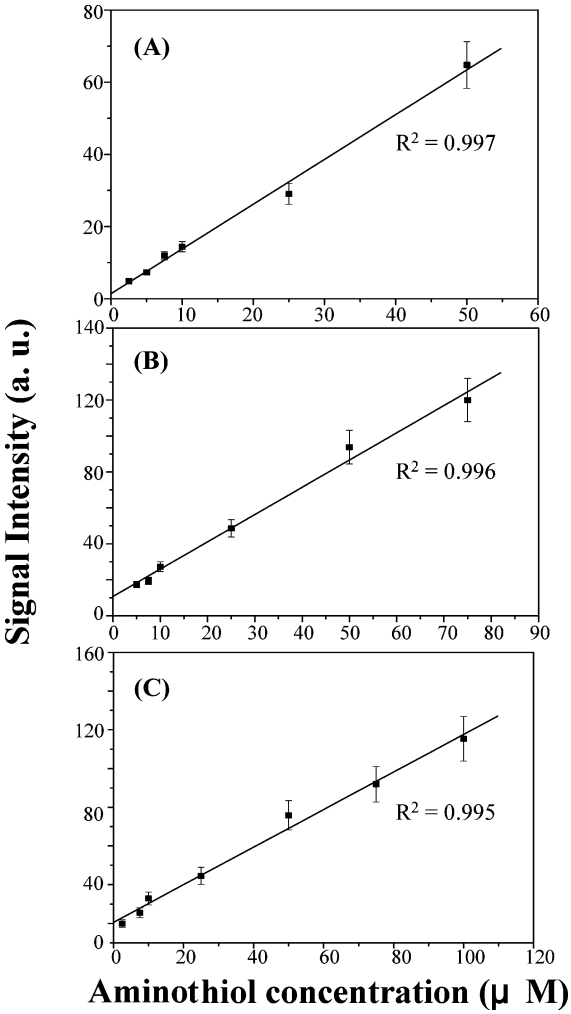

Figure 4. Calibration curves of three representative aminothiols. 14-nm-diameter (NR)AuNPs (3×) were used as matrixes for the SALDI-MS analyses. (A) $[GSH + Na]^+$, (B) $[Cys + H]^+$, and (C) $[HCys + H]^+$ ion intensities plotted as functions of aminothiol concentrations. A total of 300 pulsed laser shots were applied under a laser fluence of 52.5 μJ, except for the detection of Cys and HCys, where the laser fluence was adjusted to 66.0 μJ.

(49) Muddiman, D. C.; Gusev, A. I.; Proctor, A.; Hercules, D. M.; Venkataramanan, R.; Diven, W. *Anal. Chem.* **1994**, *66*, 2362−2368.

(50) Alterman, M. A.; Gogichayeva, N. V.; Kornilayev, B. A. *Anal. Biochem.* **2004**, *335*, 184−191.

(51) Amado, F. M. L.; Domingues, P.; Santana-Marques, M. G.; Ferrer-Correia, A. J.; Tomer, K. B. *Rapid Commun. Mass Spectrom.* **1997**, *11*, 1347−1352.

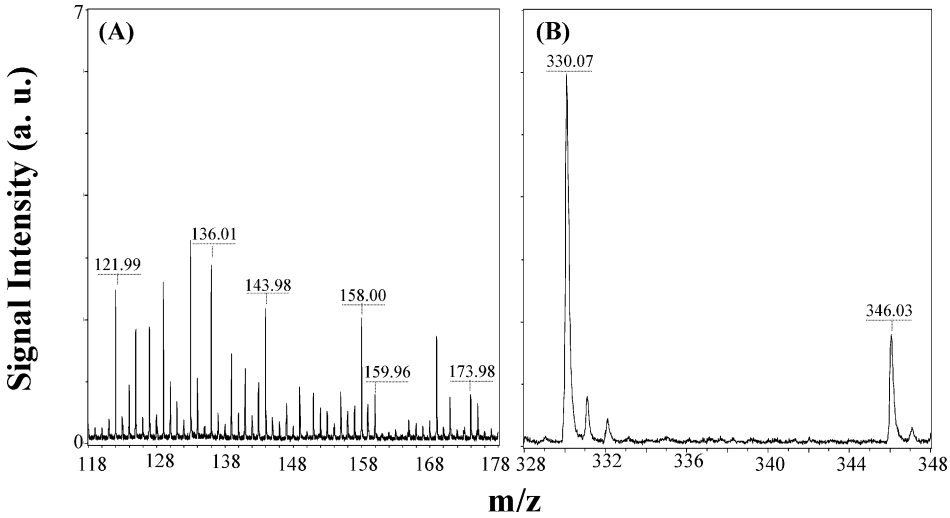

Figure 5. SALDI mass spectra of three mixed aminothiols: GSH (20.0 μM), Cys (40.0 μM), and HCys (40.0 μM). 14-nm-diameter (NR)AuNPs (3×) were used as matrixes for these SALDI-MS analyses. Peak identities: (A) *m*/*z* 121.99 $[Cys + H]^+$; *m*/*z* 143.98, $[Cys + Na]^+$; *m*/*z* 159.96, $[Cys + K]^+$; *m*/*z* 136.01, $[HCys + H]^+$; *m*/*z* 158.00, $[HCys + H]^+$; *m*/*z* 173.98 $[HCys + K]^+$; (B) *m*/*z* 330.07 and 346.03, $[GSH + Na]^+$ and $[GSH + K]^+$.

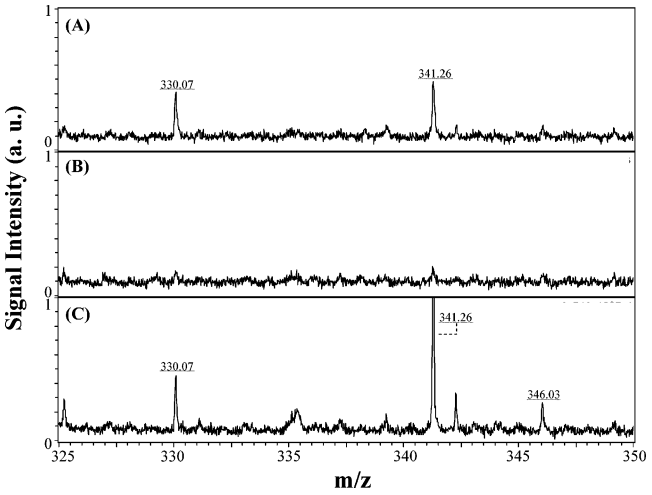

Figure 6. Mass spectra of mixtures of (A) 1.0 and (B, C) 0.1 μM GSH with (A, B) 14-nm-diameter (NR)AuNPs (3×) as matrixes without concentration of the samples and (C) 0.1× (NR)AuNPs as probes to trap 0.1 μM GSH in aqueous solution (1.0 mL) by a concentration factor of 50×. Peak identities: *m*/*z* 330.07 and 346.03, $[GSH + Na]^+$ and $[GSH + K]^+$.

efficiency for (NR)AuNPs toward GSH than toward Cys and HCys. GSH (pI = 2.86) possesses negative charges at pH 4.0, whereas Cys (pI = 5.05) and HCys (pI = 5.55) are cationic. Relative to positively charged ions, negatively charged ions more readily form (Na, K) adduct ions.[44] The spectra depicted in Figure 5 clearly indicate that we obtained high-intensity background signals in the low-mass range (m/z < 200); this situation causes a difficulty in peak assignment and poor sensitivity.

Trapping Capacity of NRAuNPs. By taking advantage of the (NR)AuNPs as selective and concentrating probes, we expected that the sensitivity of the aminothiols could be improved further in their SALDI-MS analyses.[25,28] Figure 6 provides a comparison of the peak intensities of the $[GSH + Na]^+$ and $[GSH + K]^+$ ions when performing sample preparation without (A, B) and with (C) conducting centrifugation (concentration; 6000 rpm for 10 min) of solutions containing GSH and (NR)AuNPs. Without centrifugation, as indicated in Figure 6A and B, the peaks for 1.0 μM GSH are small and we detected no peaks for 0.1 μM GSH. By using NRAuNPs (0.1×) as probes to trap GSH (0.1 μM) from a sample solution (1.0 mL), Figure 6C indicates that the peaks for the $[GSH + Na]^+$ and $[GSH + K]^+$ ions were clearly visible after concentration by a factor of 50. We assigned the peak at m/z 341.26 to $[C_{16}H_8N(C_2H_5)_2O_2 + Na]^+$, which is the sodiated NR ion. The NR molecules in the bulk solution readsorbed onto the AuNPs during centrifugation. Based on the peak heights of the signals of the $[GSH + Na]^+$ and $[GSH + K]^+$ ions in this MS spectrum, we estimated the LOD for GSH to be 25 nM. To the best of our knowledge, this value is the lowest LOD for GSH that has ever been obtained when using either SALDI-MS or MALDI-MS approaches. In two similar experiments, we achieved the LODs of 54 and 34 nM for Cys and HCys, respectively. The results indicate that the sensitivity improvements for the three aminothiols are 37−40-fold when compared to those without conducting concentration processes. Nanomaterial-based probes offer selectivity toward target molecules through a range of interactions—including electrostatic, hydrophilic, and hydrophobic interactions—to minimize any interference arising from the use of complicated matrixes prior to MALDI-MS analysis.[20d,23b,24,25] Through the use of (NR)AuNPs, we were able to concentrate and selectively trap aminothiols through the formation of Au−S interactions.

Citrate-protected (NR)AuNPs possess negative charges on their surfaces, and thus, they have the ability to bind to positively charged species in aqueous solutions through electrostatic interactions.[25,28] To test the possibility of using NRAuNPs as concentration probes and SALDI matrixes for detecting positively charged non-thiol small molecules, we applied arginine as a representative example. Arginine (pI = 10.75) molecules possess positive charges at pH values below 4.0; they were weakly attracted to the (NR)-AuNPs and did not induce aggregation (i.e., the deep-red color remained). We note that the color of the solution changed to blue-gray in the presence of GSH as a result of induced aggregation. After incubation of an aqueous solution containing GSH, arginine, and NRAuNPs for 1 h, we expected that most of the GSH

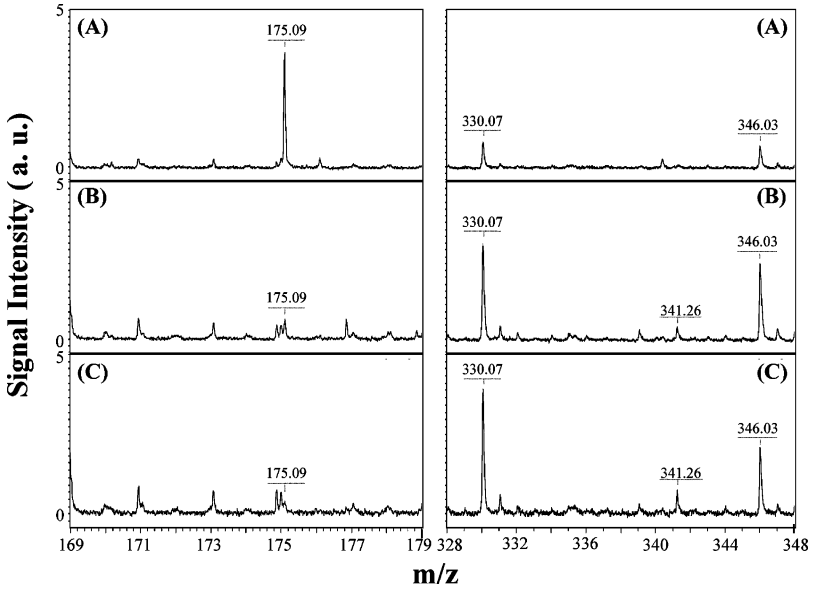

Figure 7. Mass spectra of a mixture of arginine (5.0 μM), GSH (5.0 μM), and 14-nm-diameter NRAuNPs (3×) in 0.5 mM ammonium citrate (pH 4.0). (A) Supernatant, (B) precipitate, and (C) the pellet obtained after centrifuging the mixture at 6000 rpm for 10 min. Peak identities: *m*/*z* 175.09, $[Arg + H]^+$; *m*/*z* 330.07 and 346.03, $[GSH + Na]^+$ and $[GSH + K]^+$. A total of 300 pulsed laser shots were applied under a laser fluence set at 52.5 μJ.

molecules would have adsorbed onto the (NR)AuNP surface and most of the arginine molecules would remain in the bulk solution. To support our hypothesis, we conducted SALDI-MS analyses of the bulk solution, the precipitate obtained without centrifugation, and the precipitate obtained after centrifugation of the mixture of arginine and GSH. Figure 7A indicates that, for the bulk solution, a strong peak exists for the $[Arg + H]^+$ ion (left panel) and two smaller peaks for the $[GSH + Na]^+$ and $[GSH + K]^+$ ions (right panel); in contrast, Figure 7B indicates that the peak intensity for the $[Arg + H]^+$ ion is negligible (left panel) and those for the $[GSH + Na]^+$ and $[GSH + K]^+$ ions (right panel) are strong for the sample precipitant obtained without centrifugation. The result clearly supports our spectrometric measurements (not shown) that NRAuNPs have much weaker interactions with arginine than they do with GSH. The mass spectrum in Figure 7C also displays a negligible peak for arginine (left panel), indicating that, indeed, arginine was not adsorbed onto the NRAuNPs in the bulk solution. Thus, we conclude that the reason we could detect arginine in the bulk solution in Figure 7A is because the arginine molecules were adsorbed on (NR)AuNPs during the sample drying process. Our reasoning is supported by the fact that we observed no change in the fluorescence of the (NR)AuNP solution in the presence of arginine (data not shown). On the basis of the result exhibited in Figures 5−7, we conclude that NRAuNPs offer great advantages for the concentration of small molecules and the selectivity of their analyses.

Determination of GSH, Cys, and HCys in Blood Samples. We tested the application of our proposed technique for the practical analyses of GSH, Cys, and HCys in blood samples. The mean concentration of GSH in erythrocytes (red blood cells; RBCs) is ~1 mM.[52] Figure 8A does not display an apparent peak at *m*/*z* 330.07 for the $[GSH + Na]^+$ ion when using the lysed RBC sample without removing any proteins. Large amounts of proteins, such as hemoglobin (~900 amol/cell),[53] are present in lysed RBCs. The adsorption of proteins onto the NRAuNPs caused the reduced adsorption of GSH onto the surface. In the presence of proteins, a stronger laser fluence was required for the desorption and ionization of GSH, which worsened the detection sensitivity as well as the spectral quality. To minimize the detrimental effect of proteins during the detection of GSH, we subjected the RBC samples to deproteination using 80% ACN. Figure 8B indicates that peaks for the $[GSH + Na]^+$ and $[GSH + K]^+$ ions appear clearly at *m*/*z* 330.7 and 346.3, respectively. We

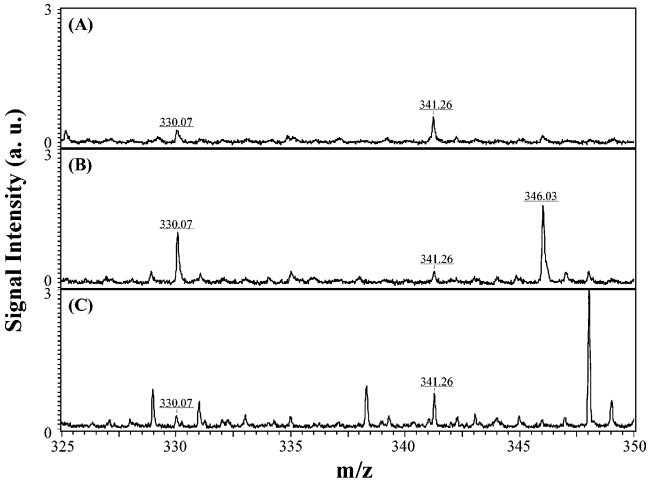

Figure 8. Mass spectra of GSH in an RBC lysate. (A) Hemoglobin-protected (NR)AuNPs (14-nm, 3×) and (B) (NR)AuNPs were used both to capture GSH in deproteined RBC lysate and as matrixes. (C) DHB was used as the matrix. The plasma samples were subjected to four cycles of centrifugation and washing and were resuspended in 0.5 mM ammonium citrate buffer (pH 4.0) prior to MS analyses. Laser shots of 300 pulses were applied under a laser fluence set at 66.0 μJ. Peak identities: *m*/*z* 330.07 and 346.03, $[GSH + Na]^+$ and $[GSH + K]^+$.

(52) Rossi, R.; Milzani, A.; Dalle-Donne, I.; Giustarini, D.; Lusini, L.; Colombo, R.; Simplicio, P. D. *Clin. Chem.* **2002**, *48*, 742−753.

(53) Moini, M.; Demars, S. M.; Huang, H. *Anal. Chem.* **2002**, *74*, 3772−3776.

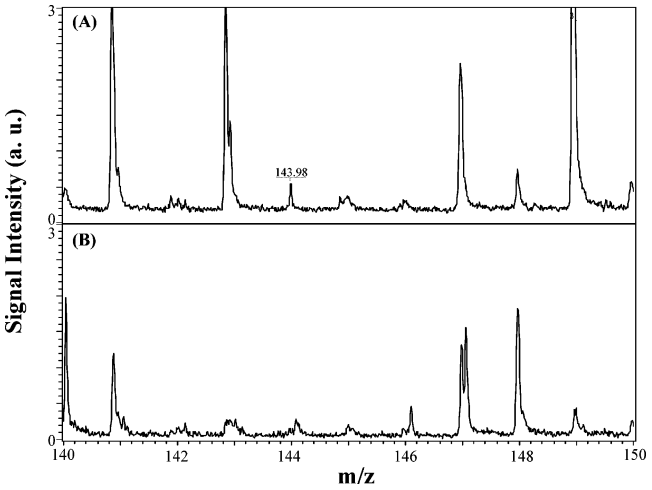

Figure 9. Mass spectra of Cys in a diluted plasma sample. (A) (NR)-AuNPs (0.1×) were used to capture Cys from deproteined plasma. (B) DHB was used as the matrix. The plasma samples were subjected to four cycles of centrifugation and washing and were resuspended in 0.5 mM ammonium citrate buffer (pH 4.0) prior to MS analyses. Laser shots of 300 pulses were applied under a laser fluence set at 66.0 μJ. The peak at m/z 143.98 is assigned to the $[Cys + Na]^+$ ion.

observed no significant changes in the background when we conducted a control experiment using the NRAuNPs treated with 80% ACN (not shown). By using a standard addition method (plotting the peak height at m/z 330.07 against the GSH concentration), we estimate that the concentration of GSH in erythrocytes is 0.79 ± 0.08 mM (n = 3); this value agrees with the normal level of between 0.70 and 0.95 mM.[52] When we used DHB as the MALDI matrix, we had difficulty in identifying any peaks for GSH (Figure 8C).

The total concentrations of GSH, Cys, and HCys in plasma are 3.71 ± 1.51, 262 ± 41, and 9.92 ± 2.99 μM, respectively.[54] Although the total concentration of Cys is relatively high, only ~5% of it exists in plasma as free Cys. Figure 9A presents the mass spectrum of Cys in the deproteined plasma sample; we used the peak at m/z 143.98 for the $[Cys + Na]^+$ ion to obtain quantitative results. After applying a standard addition, we determined that the Cys concentration in the plasma sample was 11.4 ± 1.0 μM (n = 3); this value is in good agreement with the normal levels (between 9.5 and 11.5 μM).[55] Once again, Figure 9B indicates that when we performed the MALDI-MS analysis using DHB as the matrix, we could not detect Cys in the plasma sample. Although we were able to detect GSH and Cys in the blood samples, our results indicate that the sample matrixes suppressed the signals for these two analytes; this situation leads to poor displacement and low SALDI efficiencies. In addition, the results suggested that protein-bound Cys and Hcys were not be detected by our approach. Thus, sample pretreatment is still required for complicated samples. When using the (NR)AuNPs, concentration of the biological samples also remains essential for the determination of low concentrations of analytes, such as HCys, in plasma.

(54) Carru, C.; Zinellu, A.; Sotgia, S.; Serra, R.; Usai, M. F.; Pintus, G. F.; Pes, G. M.; Deiana, L. *Biomed. Chromatogr.* **2004**, *18*, 360−366.

(55) Giuseppe, D. D.; Frosali, S.; Priora, R.; Simplicio, F. C. D.; Buonocore, G.; Cellesi, C.; Capecchi, P. L.; Pasini, F. L.; Lazzerini, P. E.; Jakubowski, H.; Simplicio, P. D. *J. Lab. Clin. Med.* **2004**, *144*, 235−245.

CONCLUSION

We prepared NRAuNPs and used them as selective probes and matrixes for the determination of GSH, Cys, and HCys through SALDI-MS. When we performed SALDI-MS analysis using the NRAuNPs, the LOD of GSH was 1.0 μM when we did not perform a concentration step and 25 nM with concentration. Although this method is not as sensitive as fluorescence measurements using NRAuNPs,[37] SALDI-MS provides very high selectivity. Using NRAuNPs as matrixes for the determination of aminothiols provides a number of advantages over DHB, including simplicity, sensitivity, selectivity, and repeatability. Because of its high selectivity toward thiol compounds, this approach results in a lower degree of matrix interference and is useful for the determination of thiol compounds in complicated biological samples after simple sample pretreatment (separation is not required). We applied our proposed method to successfully determine the levels of GSH in red blood cells and Cys in plasma samples. When applying a dual assay based on changes in both color and fluorescence, we can determine whether the aminothiol samples can be subjected to further identification and quantification through SALDI-MS; we believe that this approach may accelerate the speed of analysis when screening a number of samples.

ACKNOWLEDGMENT

This work was supported by the National Science Council (NSC 94-2113-M-002-008 and NSC 94-2113-M-002-036) of Taiwan. We thank Professor C. Y. Mou, S. T. Liu, and C. T. Chen for allowing us use of the MALDI-TOF instrument. We are grateful to L.-Y. Wang of Bruker Daltonics, Inc., and Ms. L.-J. Hwang of National Taiwan University for helpful discussion in conducting the MALDI and SALDI measurements.

Received for review October 2, 2005. Accepted November 30, 2005.

AC0517646